Available online at www.sciencedirect.com
ScienceDirect
Journal of Luminescence 128 (2008) 481–488
JOURNAL OF LUMINESCENCE
www.elsevier.com/locate/jlumin

Structure and photophysical behavior of 2,2′-bipyrimidine/lanthanide ion complexes in various environments

Vlasoula Bekiari[a], Katerina A. Thiakou[b], Catherine P. Raptopoulou[c], Spyros P. Perlepes[b], Panagiotis Lianos[a,*]

[a]*Engineering Science Department, University of Patras, 26500 Patras, Greece*
[b]*Department of Chemistry, University of Patras, 26500 Patras, Greece*
[c]*Institute of Materials Science, NCSR "Demokritos", 15310 Athens, Greece*

Received 19 March 2007; received in revised form 18 September 2007; accepted 20 September 2007
Available online 29 September 2007

Abstract

The photophysical behavior of 2,2′-bipyrimidine has been studied alone and in the presence of several lanthanide or other metal ions. This substance, which is employed as bridging ligand in homo- and hetero-dinuclear complexes, can form stable complexes with luminescent lanthanide ions like Eu^{3+} and Tb^{3+}. Complexes precipitated from common solvents are crystalline with a structure that consists of discrete, centrosymmetric dinuclear entities with a planar ligand configuration. These complexes are strongly luminescent. Luminescence is sensitized by ligand-to-metal energy transfer. However, when the ligand and metal ions are mixed in an unconventional solvent, like a poly(ethylene glycol) oligomer, all reagents stay in solution and produce a different type of complex where only an enhanced ligand-centered fluorescence can be observed. It is possible that such fluorescence is emitted by 2,2′-bipyrimidine in a non-planar configuration. This behavior has also been observed with other heterocyclic ligands that can exist in different conformers, like terpyridine, and it may explain why some ligand–lanthanide complexes sometimes fail to sensitize efficient photoluminescence.

Keywords: 2, 2′-Bipyrimidine; Lanthanide ions; Photoluminescence

1. Introduction

2,2′-Bipyrimidine (bpym) is one of the classical ligands, which are used as bridging agents in the formation of dinuclear coordination complexes. The chemical structure of coordinated bpym can be seen in Fig. 1. Its two ligation sites can bind two metal ions. In the case of luminescent lanthanide ions, they are further coordinated with other ligands, usually β-diketonates, creating interesting luminescent complexes [1–4]. As it is well known, luminescent lanthanide ions have very small light-absorption cross-section. By forming complexes with ligands, the latter become antennas, which sensitize lanthanide luminescence by ligand-to-metal energy transfer. Complexes of some transition metals with organic ligands also create interesting luminescent systems. In that case, luminescence is usually sensitized by metal-to-ligand charge transfer (MLCT) and by excitation within the visible spectrum. In this sense, dinuclear complexes, which are facilitated by bridging ligands like bpym, are studied with a lot of interest, both for making efficient and stable luminescent complexes [1] and for tailor-cutting the photophysical characteristics of the ensuing systems [2].

All studies on dinuclear complexes employing the bpym bridge accept that bpym hold a planar configuration, as derived by solid-state crystallographic data analysis. In the case of complexes with light-emitting lanthanide ions, most of the related studies deal with structures similar to the one of Fig. 1A, where the major stabilizing and sensitizing ligand is a β-diketonate. Less or no attention has been paid to binary complexes involving bpym as the only organic ligand, which can also produce equally interesting structures like the one of Fig. 1B. This structure is presented for the first time in this work. Furthermore, not much attention has been paid to the photoluminescence

*Corresponding author. Tel.: +30 2610 997513; fax: +30 61 997803.
E-mail address: lianos@upatras.gr (P. Lianos).

0022-2313/$ - see front matter © 2007 Elsevier B.V. All rights reserved.
doi:10.1016/j.jlumin.2007.09.018

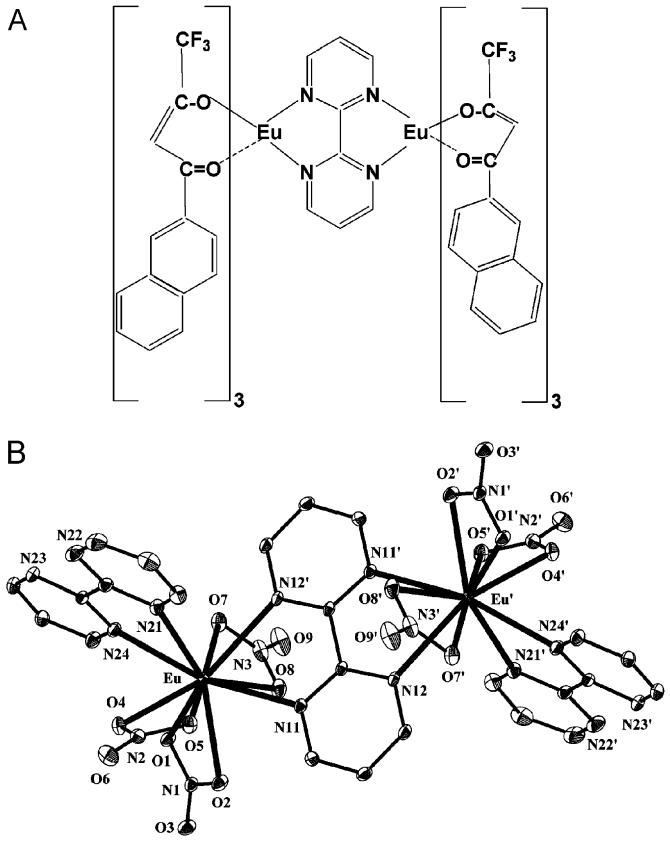

Fig. 1. (A) Structural formula of the ternary complex between 1-(2-naphthoyl)-3,3,3-trifluoroacetone, bpym, and europium(III) (cf. Ref. [1]); and (B) partially labeled ORTEP plot of the structure of the dinuclear molecule present in the complex $[Eu_2(NO_3)_6(bpym)_3]\cdot H_2O$. Primed and unprimed atoms are related by the crystallographic inversion center (symmetry operator: $-x+2$, $-y$, $-z+1$).

characteristics of bpym ligand itself. The present work attempts to fill the void. bpym is a luminescence sensitizer of lanthanide ions by itself, while the study of the possibility of conformation changes as well as the influence of various environments on bpym photophysical properties reveals unknown sides of this interesting ligand. These issues are addressed in the present work.

2. Experimental

2.1. General and physical measurements

All manipulations were performed under ambient conditions using materials and solvents as received (reagent grade; Aldrich, Alfa Aesar).

Microanalyses (C, H, N) were performed in the University of Ioannina Microanalytical Laboratory (Greece) by using an EA 1108 Carlo Erba analyzer. IR spectra (4000–500 cm^{-1}) were recorded on a Perkin-Elmer 16 PC FT spectrometer with samples prepared as KBr pellets; spectra were also recorded as Nujol and hexachlorobutadiene mulls between CsI discs. Magnetic susceptibilities were measured at room temperature using the Faraday method with a Cahn-Ventron RM-2 balance standardized with $HgCo(NCS)_4$; diamagnetic corrections were estimated from Pascal's constants. Absorption measurements were made with a Cary 1E spectrophotometer and luminescence measurements with a Cary Eclipse spectrofluorometer. Europium and terbium luminescence decay times were also measured with the Cary Eclipse spectrofluorometer. Both spectral structures and decay times were accepted as provided by the instruments without any further corrections. The instrument setting was the same for all luminescence measurements. Nanosecond decay profiles were recorded by the Photon Counting technique on a home-made apparatus employing an IBH hydrogen flash and Ortec electronics.

2.2. Compound preparation

2.2.1. $[Eu_2(NO_3)_6(bpym)_3]\cdot H_2O$

To a stirred, colorless solution of $Eu(NO_3)_3\cdot 6H_2O$ (0.087 g, 0.20 mmol) in MeCN (acetonitrile, 16 ml) was added solid bpym (0.047 g, 0.40 mmol). The solid soon dissolved and four drops of H_2O were added to the resultant pink solution. The latter was stirred for 2–3 min, and then was layered with a mixture of Et_2O and *n*-hexane (1:1 v/v, 30 ml). Slow mixing gave well-formed, X-ray quality colorless crystals of the product. The crystals were collected by filtration, washed with cold acetonitrile (5 ml) and Et_2O (2×5 ml), and dried in air. Yield: 38% (based on the metal). Found: C, 24.81; H, 1.70; N, 21.40. $C_{24}H_{20}N_{18}O_{19}Eu_2$ requires C, 24.67%; H, 1.73%; N, 21.58%. IR (KBr, cm^{-1}): 3372 sb, 3108 w, 1659 m, 1592 sh, 1576 s, 1557 m, 1504 sb, 1405 s, 1296 sb, 1206 sh, 1146 m, 1114 w, 1100 m, 1032 s, 1006 m, 827 sh, 813 m, 765 s, 749 s, 689 m, 652 s, 620 sh. μ_{eff}(BM) per metal ion: 3.39 (20 °C).

2.2.2. $[Tb_2(NO_3)_6(bpym)_3]$

Using $Tb(NO_3)_3\cdot 6H_2O$ and following exactly the same procedure as that described for the corresponding europium(III) complex, a white microcrystalline material was isolated. Yield: 21% (based on the metal). Found: C, 24.61; H, 1.63; N, 21.50. $C_{24}H_{18}N_{18}O_{18}Tb_2$ requires C, 24.75%; H, 1.56%; N, 21.79%. IR (KBr, cm^{-1}): 3393 wb, 3086 w, 1657 m, 1578 s, 1552 m, 1518 s, 1476 s, 1412 s, 1312 s, 1277 s, 1214 w, 1144 w, 1100 w, 1033 m, 1005 m, 831 w, 812 m, 764 m, 742 m, 688 m, 653 m, 621 sh. μ_{eff}(BM) per metal ion: 9.58 (22 °C).

2.3. Single-crystal X-ray crystallography

A crystal of $[Eu_2(NO_3)_6(bpym)_3]\cdot H_2O$ was mounted in air and covered with epoxy glue. Diffraction measurements were made on a Crystal Logic Dual Goniometer diffractometer using graphite-monochromated Mo radiation. Complete crystal data and parameters for data collection and processing are listed in Table 1. Unit cell dimensions were determined and refined by using the angular settings of 25 automatically centered reflections in the range

Table 1
Crystallographic data for complex $(Eu_2(NO_3)_6(bpym)_3)\cdot H_2O$

Formula	$C_{24}H_{20}Eu_2N_{18}O_{19}$
Formula weight	1168.50
Crystal color, habit	Colorless, prism
Crystal dimensions (mm)	$0.13\times0.20\times0.55$
Crystal system	Triclinic
Space group	P-1
Unit cell dimensions	
a (Å)	8.245(2)
b (Å)	7.791(2)
c (Å)	14.708(4)
α (°)	96.02(1)
β (°)	94.48(1)
γ (°)	91.87(1)
V (Å^3)	935.9(4)
Z	1
ρ_{calc} (g cm^{-3})	2.073
Radiation, λ (Å)	Mo Kα, 0.71073
Temperature (K)	298
Scan mode/speed (° min^{-1})	$\theta-2\theta$/6.0
$2\theta_{max}$ (°)	50.0
μ (mm^{-1})	3.425
Reflections collected/unique (R_{int})	3428/3298 (0.0282)
Data with $I>2\sigma(I)$	3212
Parameters refined	325
$(\Delta\rho)_{max}$, $(\Delta\rho)_{min}$ (e Å^{-3})	0.904, −0.647
Goodness-of-fit (on F^2)	1.098
R_1[a], wR_2[b] ($I>2\sigma(I)$)	0.0211, 0.0555

[a] $R_1=\sum(|F_o|-|F_c|)/\sum(|F_o|)$.
[b] $wR_2=\{\sum(w(F_o^2-F_c^2)^2)/\sum(w(F_o^2)^2)\}^{1/2}$.

$11^\circ<2\theta<23^\circ$. Three standard reflections monitored every 97 reflections showed less than 3% variation and no decay. Lorentz, polarization, and Ψ-scan absorption corrections were applied using Crystal Logic software.

The structure was solved by direct methods using SHELXS-86 [5] and refined by full-matrix least-squares techniques on F^2 SHELXL-97 [6]. All hydrogen atoms attached to carbon atoms were located by difference maps and refined isotropically; no hydrogen atoms for the solvate H_2O were included in the refinement. All non-hydrogen atoms were refined anisotropically.

The X-ray crystallographic file for $[Eu_2(NO_3)_6(bpym)_3]\cdot H_2O$ in CIF format has been deposited with the Cambridge Crystallographic Data Centre, 12 Union Road, Cambridge CB2 1EZ, UK, under the number 640681. Copies may be requested free of charge from the Director of CCDC (e-mail: deposit@ccdc.cam.ac.uk).

3. Results and discussion

3.1. Synthetic comments and conventional characterization

The 1:2 reaction between $Eu(NO_3)_3\cdot6H_2O$ and bpym in acetonitrile gave a pale pink solution; layering of this solution with Et_2O/*n*-hexane gave complex $[Eu_2(NO_3)_6(bpym)_3]\cdot H_2O$ in moderate yield. The formation of this complex can be summarized in the balanced Eq. (1). The "wrong" reaction ratio employed for the preparation of $[Eu_2(NO_3)_6(bpym)_3]\cdot H_2O$, compared to

$$2Eu(NO_3)_3\cdot6H_2O+3bpym\xrightarrow{MeCN}[Eu_2(NO_3)_6(bpym)_3]\cdot H_2O+11H_2O \quad (1)$$

the stoichiometric ratio required by Eq. (1), obviously did not prove detrimental to the formation of the complex. With the identity of $[Eu_2(NO_3)_6(bpym)_3]\cdot H_2O$ crystallographically established (vide infra), the "correct" stoichiometric ratio, i.e. Eu^{III}:bpym = 1:1.5, was employed and led to the pure compound. This complex seems to be the only isolable product from the $Eu(NO_3)_3\cdot6H_2O$/bpym reaction system. The Eu^{III} to ligand reaction ratio (we used 1:3 ratios to "force" the formation of mononuclear complexes, e.g. $[Eu(NO_3)_3(bpym)_x]$ with $x=2$ or 3), the presence of counter-cations or -anions (we added $Bu^n_4N^+$ or ClO_4^- in some reaction mixtures to "force" the isolation of ionic complexes), the nature of the solvent (use of alcohols gives the same product) and the precipitation/crystallization method have no influence on the identity of the product.

The terbium (III) complex $[Tb_2(NO_3)_6(bpym)_3]$ was prepared and isolated in a completely analogous manner. Analytical data repeatedly indicated the empirical formula $Tb(NO_3)_3\cdot1.5\,bpym$. The IR spectrum of the Tb^{III} compound is very similar to that of $[Eu_2(NO_3)_6(bpym)_3]\cdot H_2O$, with the exception of the H_2O bands which are absent in the former. The absence of lattice H_2O from $[Tb_2(NO_3)_6(bpym)_3]$ is probably due to its polycrystalline character. The spectral similarity of the two complexes is a strong evidence that the Tb^{III} complex has a molecular structure similar to that of $[Eu_2(NO_3)_6(bpym)_3]\cdot H_2O$ (vide infra).

The gadolinium(III) analoge of $[Eu_2(NO_3)_6(bpym)_3]\cdot H_2O$, i.e. complex $[Gd_2(NO_3)_6(bpym)_3]\cdot H_2O$, was also prepared [7] to be used for comparison and for the detection of the triplet emission of bpym (see below). It is isostructural with $[Eu_2(NO_3)_6(bpym)_3]\cdot H_2O$ as proved by its unit cell determination: triclinic, *P*-1, $a=8.233(4)$ Å, $b=7.789(4)$ Å, $c=14.667(8)$ Å, $\alpha=96.16(2)^\circ$, $\beta=94.51(1)^\circ$, $\gamma=91.65(2)^\circ$, $V=931.6(4)$ Å^3, $Z=1$.

The $\nu(C\cdots C)$ and $\nu(C\cdots N)$ vibrations of free bpym at 1565, 1556, 1432, and 1404 cm^{-1} shift to higher frequencies in $[Eu_2(NO_3)_6(bpym)_3]\cdot H_2O$, $[Tb_2(NO_3)_6(bpym)_3]$, and $[Gd_2(NO_3)_6(bpym)_3]\cdot H_2O$ due to coordination. The appearance of three bands in the 1600–1500 cm^{-1} in the spectra of the complexes is indicative of the presence of both chelating and bridging bpym ligands [8]. The nitrate vibrations in the IR spectra of the three complexes confirm $[(Eu_2(NO_3)_6(bpym)_3]\cdot H_2O)$ or suggest $[(Tb_2(NO_3)_6(bpym)_3]$ and $[Gd_2(NO_3)_6(bpym)_3]\cdot H_2O)$ the presence of bidentate chelating nitrato ligands since the separation of the two highest frequency bands $\nu_1(A_1)$ ($\nu(N{=}O)$) and $\nu_5(B_2)$ ($\nu_{as}(NO_2)$) under C_{2v} symmetry, appeared at 1500–1520 and 1296–1312 cm^{-1}, respectively, is large (~200 cm^{-1}) [9].

The experimental, room-temperature effective magnetic moment (μ_{eff}) values per Ln^{III} ion for $[Eu_2(NO_3)_6(bpym)_3]\cdot H_2O$ and $[Tb_2(NO_3)_6(bpym)_3]$ (see Section 2.2) show very little deviation from the theoretical values (Eu^{III}, 3.5 BM; Tb^{III}, 9.7 BM) predicted by Eq. (2), suggesting that the 4f electrons in the complexed Ln^{III} ions are well-shielded by the outermost 5s and 5p electrons [10].

$$\mu_{eff} = g[J(J+1)]^{1/2} \quad (2)$$

3.2. Description of structure

A partially labeled plot of the dinuclear molecule present in complex $[Eu_2(NO_3)_6(bpym)_3]\cdot H_2O$ is shown in Fig. 1B. The coordination polyhedron of the Eu^{III} ion is shown in Fig. 2. Selected interatomic distances and angles are listed in Table 2.

The crystal structure of $[Eu_2(NO_3)_6(bpym)_3]\cdot H_2O$ consists of discrete, centrosymmetric dinuclear $[Eu_2(NO_3)_6(bpym)_3]$ molecules and solvent H_2O molecules; the latter will not be further discussed. In the dinuclear molecule, the two Eu^{III} centers are bridged by one bis-bidentate bridging (η^2:η^2:μ) bpym ligand. One chelating bpym molecule (η^2) and three nearly symmetrical planar nitrate ions complete 10-coordination at each metal ion. The crystallographic inversion center is the midpoint of the inter-ring carbon–carbon bond of the bridging bpym ligand.

The Eu–N bond distances for the bridging bpym (2.644(3), 2.658(3) Å) are longer than the Eu–N(21, 24) distances (2.564(3), 2.585(3) Å) exhibited by the terminal bpym ligand. The bite angle of the terminal bpym ligand (62.8(1)°) is slightly longer than that observed for the bridging one (61.1(1)°) in accordance [8] with the different Eu–N bond distances involved. The Eu–O (nitrato) bond lengths are in the narrow 2.447(2)–2.508(2) Å. The nitrato ligands are planar, as indicated by the sum of O–N–O angles (359.9–360.0°), and almost symmetrically chelated. The slight differences between bond distances and angles of terminal and bridging bpym ligands are due to their different coordination modes [11]. The carbon–carbon inter-ring bond lengths in $[Eu_2(NO_3)_6(bpym)_3]\cdot H_2O$ (1.479(5), 1.492(6) Å) are practically identical to the corresponding bond length in free bpym (1.502 Å) and bpym · $2H_2O$ (1.497 Å) in the solid state [12]. Each bpym group is planar; the dihedral angle between the pyrimidine rings of the terminal bpym ligand is 2.4°, where the pyrimidine rings of the bridging bpym group are strictly coplanar (angle 0.0°) due to symmetry. The chelating bpym ligands are strictly parallel (as required by symmetry) and nearly perpendicular to the plane of the bridging bpym ligand, the angle between their least-squares planes being 72.2°.

Table 2
Selected interatomic distances (Å) and bond angles (°) for complex $[Eu_2(NO_3)_6(bpym)_3]\cdot H_2O$

Eu···Eu′[a]	6.919(1)	N(1)–O(1)	1.259(3)
Eu–O(1)	2.464(2)	N(1)–O(2)	1.273(3)
Eu–O(2)	2.508(2)	N(1)–O(3)	1.207(3)
Eu–O(4)	2.447(2)	N(2)–O(4)	1.268(4)
Eu–O(5)	2.491(2)	N(2)–O(5)	1.273(4)
Eu–O(7)	2.496(3)	N(2)–O(6)	1.204(4)
Eu–O(8)	2.498(3)	N(3)–O(7)	1.273(4)
Eu–N(21)	2.585(3)	N(3)–O(8)	1.261(4)
Eu–N(24)	2.564(3)	N(3)–O(9)	1.214(4)
Eu–N(11)	2.658(3)	C(21)[b]–N(21)	1.337(5)
Eu–N(12′[a])	2.644(3)	C(24)[b]–N(21)	1.350(4)
O(1)–Eu–O(2)	51.3(1)	O(4)–Eu–O(7)	131.5(1)
O(4)–Eu–O(5)	51.6(1)	O(5)–Eu–O(7)	172.0(1)
O(7)–Eu–O(8)	51.0(1)	O(2)–Eu–N(24)	121.6(1)
N(21)–Eu–N(24)	62.8(1)	O(8)–Eu–N(21)	142.1(1)
N(11)–Eu–N(12′[a])	61.1(1)	N(11)–Eu–N(24)	165.2(1)

[a]Primes are used for atoms generated by the crystallographic inversion center (symmetry operation: $-x+2$, $-y$, $-z+1$).
[b]These carbon atoms have not been labeled in Fig. 1.

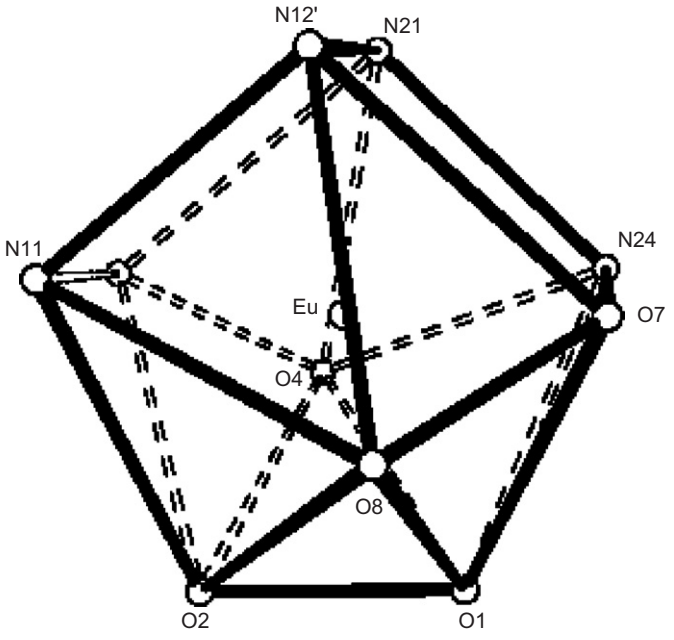

Fig. 2. A view of the inner coordination polyhedron of $[Eu_2(NO_3)_6(bpym)_3]\cdot H_2O$ showing the tetradecahedral coordination of the Eu^{III} ion. The primes indicate the symmetry operation $-x+2$, $-y$, $-z+1$.

Of the accessible, 10-coordinate polyhedra for [M(bidentate ligand)$_5$] systems [13], i.e. bicapped square antiprism, sphenocorona, pentagonal antiprism and tetracapped trigonal prism, the sphenocorona (tetradecahedron) is the most appropriate for the description of the 10 donor atoms in $[Eu_2(NO_3)_6(bpym)_3]\cdot H_2O$, see Fig. 2.

There are no stacking interactions in the crystal lattice. Although the hydrogen atoms of the lattice H_2O molecule (O(10)) were not included in the crystal structure refinement, the short O(10)···O(8) and O(10)···O(7) ($-x+2$, $-y+1$, $-z+1$) distances of 2.831 and 3.016 Å, respectively, raise the possibility of the presence of hydrogen bonds; if this is real, the dimers form chains along the *b*-axis.

Complex $[Eu_2(NO_3)_6(bpym)_3]\cdot H_2O$ joins a very small family of structurally characterized *homometallic*, i.e. containing exclusively Ln^{III} ions, lanthanide(III)/2,2′-bipyrimidine complexes. The three reported complexes were all Eu^{III} complexes, i.e. $[Eu_2(NTA)_6(bpym)]$ [1], where NTA^- is 1-(2-naphthoyl)-3,3,3-trifluoroacetonate, $[Eu_2(dbm)_6(bpym)]$ [4], where dbm^- is the dibenzoylmethanate ligand, and $[Eu_2(tta)_6(bpym)]$ [4], where tta^- is the theonyltrifluoroacetonate ligand. In these three complexes, the bpym ligand is bridging and the Eu^{III} centers are eight-coordinate. Thus, $[Eu_2(NO_3)_6(bpym)_3]\cdot H_2O$ is the first such complex that comprises both terminal and bridging bpym ligands. It should be mentioned at this point that *hetero-metallic* d-/4f-metal/bpym complexes have also been structurally characterized; these are $[Re(CO)_3Cl(\mu\text{-bpym})Ln(fod)_3]$ [2,14], where fod^- is $CF_3CF_2CF_2C(O)CHC(O)^tBu^-$ and Ln = Er, Yb, $[MNd(bpym)(H_2O)_4(CN)_6]_n$ [15], where $M^{III} = Fe^{III}$, Co^{III}, and $[(F_3C\text{–}C_6H_4\text{–}CC)_2Pt(\mu\text{-bpym})Ln(hfac)_3]$ [2], where $hfac^-$ is the hexafluoroacetylacetonate ligand and Ln = Gd, Nd.

3.3. Photoluminescence studies

The photophysical characteristics of the bpym ligand have been studied in low- and high-concentrated solutions in various solvents and the data are shown in Fig. 3. Fig. 3A shows absorption, excitation, and fluorescence spectra of a low-concentrated (10^{-6} M) solution of bpym in tetrahydrofuran (THF). Absorption and excitation was structured in two UV peaks while fluorescence contained a single peak at 350 nm. These spectra correspond to the π–π* transition [3]. Fig. 3B shows spectra of high-concentrated (10^{-3} M) bpym solutions in THF. The absorption (not shown) was similar to the one recorded with low-concentrated solution, thus excluding formation of aggregates. The π–π* fluorescence, peaking at 350 nm, was now substantially quenched. Thus, the peak intensity of the corresponding curve #1 in Fig. 3B was less than half of the corresponding peak intensity of curve #3 in Fig. 3A, both spectra obtained by excitation at 320 nm. Furthermore, a new weak fluorescence band with a long tail and a maximum at 448 nm appeared. The decrease of the intensity of the π–π* fluorescence is obviously due to quenching by self-absorption, as it usually happens with concentrated solutions. The excitation corresponding to the new fluorescence band was very different from the excitation of the π–π* band in both structure and position. Thus, it practically contained a single peak and it was now centered around 356 nm. Obviously this new emission comes from a weak n–π* transition (cf. Ref. [3]). Similar behavior was previously reported for terpyridine [16]. When bpym was dissolved in other solvents like ethanol or polyethyleneglycol-200 (PEG200), it demonstrated the same behavior as in THF solutions. Studies were carried out in PEG200 solutions because, as it will be seen below, this solvent induces a particular behavior to the bpym–metal complexes.

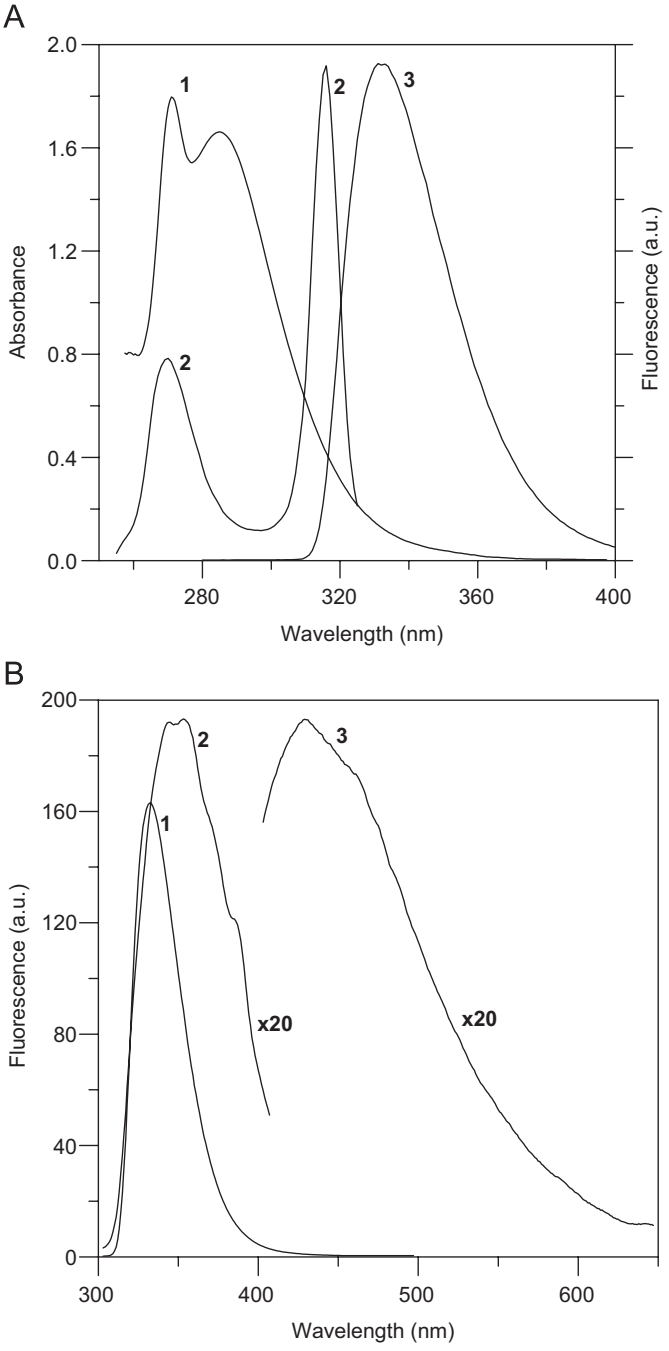

Fig. 3. (A) Absorption (1), excitation (Em.wl. 350 nm) (2), and fluorescence (Exc.wl. 320 nm) (3) spectrum of 10^{-6} M bpym in THF. (B) Fluorescence (Exc.wl. 320 nm) (1), excitation (Em.wl. 448 nm) (2), and fluorescence (Exc.wl. 356 nm) (3) spectrum of 10^{-3} M bpym in THF.

Complexes of bpym with Eu^{3+}, Tb^{3+}, or Gd^{3+} have been isolated by precipitation from acetonitrile solutions (see Section 2). As already said, the crystal structure consists of the entities shown in Fig. 1B. It is seen that bpym holds a planar configuration. The photophysical characteristics of these complexes are shown in Fig. 4. Fig. 4A shows the excitation and emission spectrum of $[Eu_2(NO_3)_6(bpym)_3]\cdot H_2O$ and Fig. 4B of $[Tb_2(NO_3)_6(bpym)_3]$. For both complexes, the spectra are characteristic

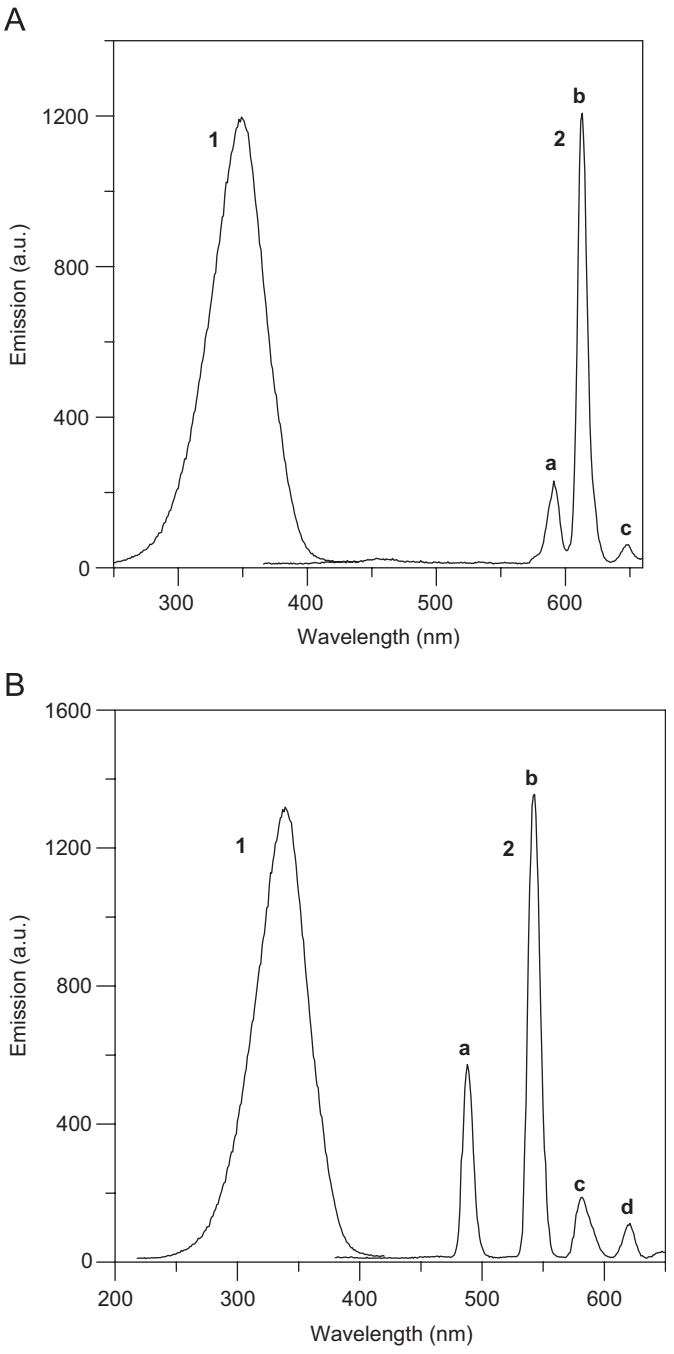

Fig. 4. Excitation (1) and emission (2) spectra of the solid complexes: (A) $[Eu_2(NO_3)_6(bpym)_3]\cdot H_2O$ and (B) $[Tb_2(NO_3)_6(bpym)_3]$. Assignment of emission peaks: (A) a: $^5D_0\rightarrow{}^7F_{0,1}$; b: $^5D_0\rightarrow{}^7F_2$; c: $^5D_0\rightarrow{}^7F_3$; (B) a: $^5D_4\rightarrow{}^7F_6$; b: $^5D_4\rightarrow{}^7F_5$; c: $^5D_4\rightarrow{}^7F_4$; d: $^5D_4\rightarrow{}^7F_3$. The excitation wavelength was 342 nm in both cases. The emission wavelength for recording excitation spectra was 613 nm in (A) and 542 nm in (B).

of intense metal-centered emission obtained by ligand-centered excitation and ligand-to-metal energy transfer. The corresponding decay times were 0.63 ($\pm$0.02) ms and 0.76 ($\pm$0.02) ms for $[Eu_2(NO_3)_6(bpym)_3]\cdot H_2O$ and $[Tb_2(NO_3)_6(bpym)_3]$, respectively. For measuring these decay times the emission was monitored at 613 nm ($^5D_0\rightarrow{}^7F_2$ transition, i.e. the highest peak in luminescence spectrum of Fig. 4A) and 542 nm ($^5D_4\rightarrow{}^7F_5$ transition, i.e. the highest peak in luminescence spectrum of Fig. 4B) for europium and terbium complexes, respectively. As expected, the complex with Gd^{3+} did not produce any metal-centered emission since the emissive state of Gd^{3+} is too high to accept energy transfer. Indeed, this state ($^6P_{7/2}$) lies at $>30.000\,cm^{-1}$ [17], while that of Eu^{3+} ($^5D_0$) lies at $17250\,cm^{-1}$ [18] and that of Tb^{3+} ($^5D_4$) at $20500\,cm^{-1}$ [19]. The complex with Gd^{3+} can be employed to determine the triplet state of bpym [20]. We have tried to record the triplet state emission at low temperature but it was very weak and it was impossible to record it accurately. It is, however, logical to accept that the triplet state simply lies at a wavelength compatible with the above $^5D_4$ and $^5D_0$ states for Tb^{3+} and Eu^{3+}, respectively, i.e. somewhere within the blue–green spectral window. The crystals of $[Ln_2(NO_3)_6(bpym)_3]$ complexes (Ln = Eu or Tb) can be dissolved in THF. In that case, the dissolved complexes also gave lanthanide emission by ligand-to-metal energy transfer. However, the complexes were in that case partly dissociated so that a weak π–π^* fluorescence was also produced by dissociated ligand.

When bpym and metal ions were mixed in PEG200, the system demonstrated a different photophysical behavior. Liquid polyethylene glycol oligomers have been found in previously studied cases [16,21,22] to have a particular behavior that distinguishes them from other solvents. Pure PEG200 is optically inactive. PEG200 dissolves both bpym and metal ions and has the ability to form weak complexes with both. For this reason, the Ln–bpym complex discussed so far was not detected in PEG200. Fig. 5 shows absorption, excitation, and emission spectrum of the bpym–Eu^{3+}–PEG200 mixture. The absorption spectrum was different from that of pure bpym in various common

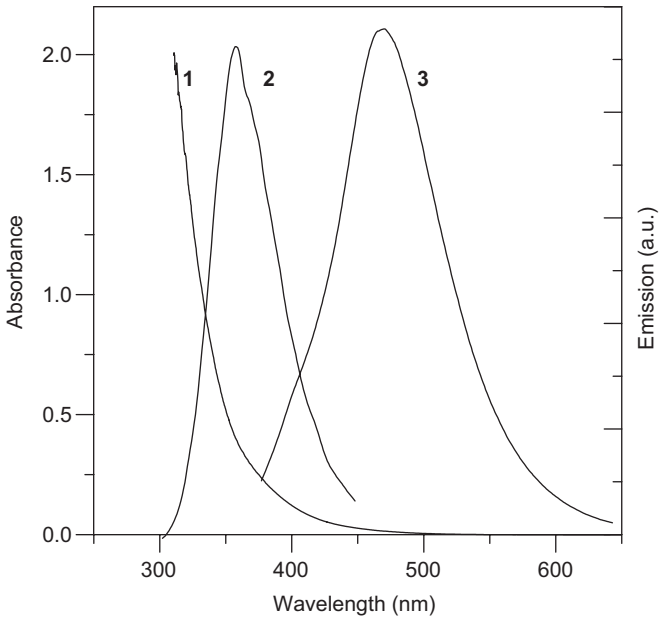

Fig. 5. Absorption (1), excitation (Em.wl. 470 nm) (2), and emission (Exc.wl. 356 nm) (3) of the mixture Eu^{3+}/bpym/PEG200. The concentration of both Eu^{3+} and bpym was 10^{-3} M.

solvents or in PEG200 itself, as represented by curve #1 of Fig. 3A. This means that when Eu^{3+} and bpym find themselves close to each other in PEG200, they interact and form a complex that dramatically changes light-absorption characteristics. Curve #1 of Fig. 5 has a long tail that deeply extends into the visible, up to about 500 nm. Whatever this complex is, it has to be different from the solid complex obtained by precipitation from various common solvents, since the emission spectrum is not metal-centered and it is not characteristic of Eu^{3+}. The emission spectrum represented by curve #3 of Fig. 5 is ligand-centered, it is relatively intense and is independent of the complexed metal. Indeed, the intensity of the emission corresponding to curve #3 of Fig. 5 is 80 times stronger than the intensity corresponding to curve #3 of Fig. 3B, both recorded by excitation at the same wavelength. Exactly the same emission was recorded when bpym was mixed in PEG200 with Tb^{3+}, Gd^{3+}, In^{3+} or other trivalent or divalent metal ions. The emission maximum lies at 470 nm. Its excitation spectrum consists of a single band with a maximum located at 356 nm. The origin of this ligand-centered emission band is not obvious. We can be led to some conclusions by excluding various possibilities. This emission is not a triplet emission (i.e. phosphorescence), even though it lies in the same spectral area, because it has a very short decay time (about 5 ns) and relatively high intensity. The phosphorescence observed in the case of the $[Gd_2(NO_3)_6(bpym)_3]\cdot H_2O$ complex was extremely weak and was hardly detected even at very low temperature. The above emission is not an MLCT either. MLCT also induces a very weak luminescence with much longer lifetime. In addition, if it were an MLCT emission, it should depend on the complexed metal, which is not the present case. It is then concluded that the 470 nm emission is fluorescence, possibly, emitted by a different bpym conformer, i.e. by a non-planar configuration. This fluorescence was excited exactly at 356 nm, which corresponds to a n–π^* excitation. An analogous conclusion was previously drawn for the case of 2,2′:6′,2″-terpyridine [16]. It seems that PEG200 allows for keeping bpym and metal ions in suspension even after complex has been formed between them, thanks to the affinity that PEG200 has for both ligand and metal ion thanks to its ether oxygens. The complex between the ligand and the metal ion is possibly obtained with participation of PEG200 molecules. It is a complex that does not allow ligand-to-metal energy transfer, possibly because bpym is at a different conformation. Thus, only ligand-centered fluoresence can be produced. Naturally, since bpym concentration is in that case high, i.e. 10^{-3} M, the n–π^* transition at 356 nm is the prevalent excitation mode. The above blue-green fluorescence is not a n–π^* fluorescence. This is supported by the following two arguments. First, it peaks at a different wavelength from the n–π^* fluorescence of Fig. 3B. Indeed, it peaks at 470 nm while that of curve #3 of Fig. 3B peaks at 448 nm. Second, it is a relatively intense emission, much stronger than that of curve #3 Fig. 3B (i.e. 80 times stronger), the two emissions been excited at the same wavelength (356 nm). Finally, this new emission is not due to a solvatochromic (solvent polarity) effect since the free bpym fluorescence spectra, as already mentioned, did not change in going from THF to ethanol of PEG200. Conformational changes appear as the most plausible explanation for the origin of this new emission. Evidence for the non-planarity of the two pyrimidine rings of free bpym has actually been presented in the past. The structure of bpym was determined in the gas phase by the Electron Diffraction method [12]. The torsion angle about the inter-ring bond was found to be 49° in the gas phase using a static model. When a dynamic model was applied, the energy barriers at 0° and 90° in the twist angle were found to be 6.3 and 2.5 kJ mol^{-1}, with the energy minimum at 48°. In the single-crystal, X-ray structure of bpym [12] the two rings are forced by symmetry to be coplanar. However, the libration about the long axis of the molecule is large, which may correspond to a statistically disordered non-planar molecule [12]. Although the individually planar pyrimidine rings of the bpym ligands in $[Eu_2(NO_3)_6(bpym)_3]\cdot H_2O$ (and most probably in $[Tb_2(NO_3)_6(bpym)_3]$ and the Gd^{III} complex) are strictly (the bridging bpym) or almost (the terminal bpym) coplanar, the situation may be different in unconventional solvents.

4. Conclusions

2,2′-Bipyrimidine can form complexes with various lanthanide and other metal ions. In common solvents, a mixture of bpym and lanthanide ions leads to the formation of solid $[Ln_2(NO_3)_6(bpym)_3]$ complexes. These ligand–lanthanide complexes are based on a planar ligand configuration, as deduced from crystallographic data. They can be excited in the near UV and they can sensitize strong metal-centered luminescence by ligand-to-metal energy transfer. However, when bpym and various metal ions are mixed in an unconventional solvent, like PEG200 or other poly(ethylene glycol) oligomers, which are in the liquid phase, they remain in suspension and form a different type of complex, where a non-planar configuration of the ligand may possibly be involved. These complexes do not sensitize metal-centered luminescence but produce a relatively intense ligand-centered fluorescence, completely independent of the complexed ion. An analogous phenomenon was observed with 2,2′:6′,2″-terpyridine [16], a ligand that can also form different conformers. This phenomenon must be taken into account in the studies of ligand–lanthanide luminescent complexes because it may explain the failure to produce efficient sensitizers of lanthanide luminescence in some cases.

References

[1] J.A. Fernandes, R.A. Sa Ferreira, M. Pillinger, L.D. Carlos, J. Jepsen, A. Hazell, P. Ribeiro-Claro, I.S. Goncalves, J. Lumin. 113 (2005) 50.

[2] N.M. Shavaleev, G. Accorsi, D. Virgili, Z.R. Bell, T. Lazarides, G. Calogero, N. Armaroli, M.D. Ward, Inorg. Chem. 44 (2005) 61.
[3] R. Sultan, K. Gadamsetti, S. Swavey, Inorg. Chim. Acta 359 (2006) 1233.
[4] H. Jang, C.-H. Shin, B.-J. Jung, D. Kim, H.-K. Shim, Y. Do, Eur. J. Inorg. Chem. (2006) 718.
[5] G.M. Sheldrick, SHELXS-86, Structure Solving Program, University of Göttingen, Germany, 1986.
[6] G.M. Sheldrick, SHELXL-97, Program for the Refinement of Crystal Structures from Diffraction Data, University of Göttingen, Germany, 1997.
[7] No details are given here because this compound will be incorporated into a full paper dealing with the magnetic properties of bpym-bridged, dinuclear lanthanide (III) complexes.
[8] G. De Munno, G. Viau, M. Julve, F. Lloret, J. Fauss, Inorg. Chim. Acta 257 (1997) 121.
[9] K. Nakamoto, Infrared and Raman Spectra of Inorganic and Coordination Compounds, fourth ed., Wiley, New York, 1986, pp. 254–257.
[10] S. Liu, L. Gelmini, S.J. Rettig, R.C. Thompson, C. Orvig, J. Am. Chem. Soc. 114 (1992) 6081.
[11] G. De Munno, M. Julve, M. Verdaguer, G. Bruno, Inorg. Chem. 32 (1993) 2215.
[12] L. Fernholt, C. Rømming, S. Samdal, Acta Chem. Scand. A 35 (1981) 707.
[13] D.L. Kepert, Inorganic Stereochemistry, Springer, Berlin, 1982, pp. 188–193.
[14] N.M. Shavaleev, Z.R. Bell, M.D. Ward, J. Chem. Soc., Dalton Trans. (2002) 3925.
[15] B.-Q. Ma, S. Gao, G. Su, G.-X. Xu, Angew. Chem. Int. Ed. 40 (2001) 434.
[16] V. Bekiari, P. Lianos, Langmuir 22 (2006) 8602.
[17] I. Hemmila, J. Alloys Compd. 225 (1995) 480.
[18] M. Dejneka, E. Snitzer, R.E. Riman, J. Non-Cryst. Solids 202 (1996) 23.
[19] B.C. Joshi, J. Non-Cryst. Solids 180 (1995) 217.
[20] N. Weibel, L.J. Charbonniere, M. Guarigli, A. Roda, R. Ziessel, J. Am. Chem. Soc. 126 (2004) 4888.
[21] V. Bekiari, P. Lianos, Adv. Mater. 10 (1998) 1455.
[22] V. Bekiari, G. Pistolis, P. Lianos, Chem. Mater. 11 (1999) 3189.